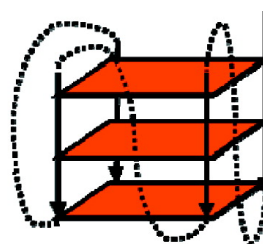
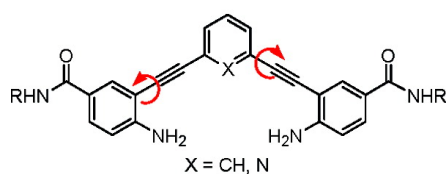


Diarylethynyl Amides That Recognize the Parallel Conformation of Genomic Promoter DNA G-Quadruplexes

Jyotirmayee Dash, Pravin S. Shirude, Shang-Te Danny Hsu, and Shankar Balasubramanian

J. Am. Chem. Soc., **2008**, 130 (47), 15950-15956 • DOI: 10.1021/ja8046552 • Publication Date (Web): 04 November 2008

Downloaded from <http://pubs.acs.org> on February 8, 2009



More About This Article

Additional resources and features associated with this article are available within the HTML version:

- Supporting Information
- Access to high resolution figures
- Links to articles and content related to this article
- Copyright permission to reproduce figures and/or text from this article

[View the Full Text HTML](#)

Diarylethynyl Amides That Recognize the Parallel Conformation of Genomic Promoter DNA G-Quadruplexes

Jyotirmayee Dash, Pravin S. Shirude, Shang-Te Danny Hsu, and Shankar Balasubramanian*

The University Chemical Laboratory, University of Cambridge, Lensfield Road, Cambridge, CB2 1EW, U.K.

Received June 26, 2008; E-mail: sb10031@cam.ac.uk

Abstract: We report bis-phenylethynyl amide derivatives as a potent G-quadruplex binding small molecule scaffold. The amide derivatives were efficiently prepared in 3 steps by employing Sonogashira coupling, ester hydrolysis and a chemoselective amide coupling. Ligand-quadruplex recognition has been evaluated using a fluorescence resonance energy transfer (FRET) melting assay, surface plasmon resonance (SPR), circular dichroism (CD) and ^1H nuclear magnetic resonance (NMR) spectroscopy. While most of the G-quadruplex ligands reported so far comprise a planar, aromatic core designed to stack on the terminal tetrads of a G-quadruplex, these compounds are neither polycyclic, nor macrocyclic and have free rotation around the triple bond enabling conformational flexibility. Such molecules show very good binding affinity, excellent quadruplex:duplex selectivity and also promising discrimination between intramolecular promoter quadruplexes. Our results indicate that the recognition of the c-kit2 quadruplex by these ligands is achieved through groove binding, which favors the formation of a parallel conformation.

Introduction

Genomic G-quadruplex forming nucleic acids have generated considerable recent interest as prospective targets for chemical intervention of biological function.¹ G-rich sequences are found in the telomeres at the chromosome ends,² and telomere binding proteins can control the G-quadruplex formation *in vivo*.³ Small molecules that selectively bind G-quadruplex DNA can inhibit the enzymatic action of telomerase⁴ and interfere with telomere function.⁵ G-quadruplex sequence motifs are widespread throughout the genome⁶ and are particularly enriched in gene promoters.^{7–9} Promoter quadruplexes associated with proto-oncogenes that have been characterized include c-myc,^{7a} c-kit,⁸

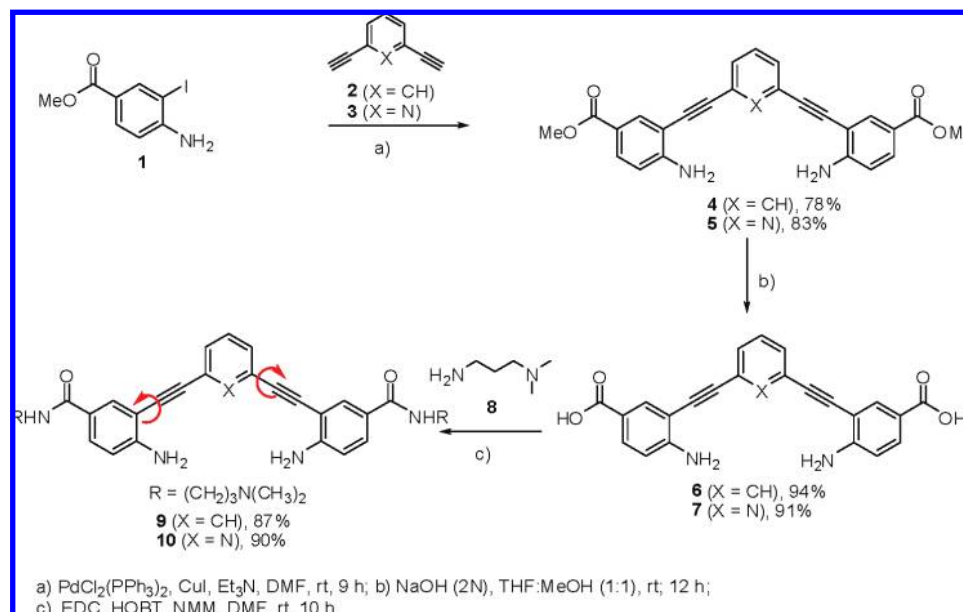
and KRAS,^{9a} and for each of these cases there is evidence that the binding of small molecules to the associated G-quadruplex can modulate transcription.^{7,9}

Furthermore, small molecule-G-quadruplex recognition is currently being explored for creating nanomolecular devices¹⁰ and developing nucleic acid based catalysis.¹¹ Most G-quadruplex ligands reported so far comprise a planar, aromatic core designed to stack on the terminal tetrads of a G-quadruplex.¹² Examples include polyaromatic hydrocarbons and conformationally constrained macrocyclic frameworks.¹² Given that many

- (1) (a) Davis, J. *Angew. Chem., Int. Ed.* **2004**, *43*, 668. (b) Burger, A. M.; Dai, F.; Schultes, C. M.; Reszka, A. P.; Moore, M. J. B.; Double, J. A.; Neidle, S. *Cancer Res.* **2005**, *65*, 1489. (c) Mandine, E.; Riou, J.-F.; Mergny, J.-L.; Mailliet, P.; Boussin, F. *Oncogene* **2005**, *24*, 2917. (d) Han, H.; Hurley, L. H. *TIPS* **2000**, *21*, 136. (e) Qin, Y.; Hurley, L. H. *Biochimie* **2008**, *90*, 1149.
- (2) Sen, D.; Gilbert, W. *Nature* **1990**, *344*, 410.
- (3) Paeschke, K.; Simonsson, T.; Postberg, J.; Rhodes, D.; Lipps, H. *J. Nat. Struct. Mol. Biol.* **2005**, *12*, 847.
- (4) (a) Cerone, M. A.; Londono-Vallejo, J. A.; Autexier, C. *Oncogene* **2006**, *25*, 7411. (b) Gomez, D.; Paterski, R.; Lemarteleur, T.; Shin-ya, K.; Mergny, J.-L.; Riou, J.-F. *J. Biol. Chem.* **2004**, *279*, 41487.
- (5) (a) Gomez, D.; Wenner, T.; Brassart, B.; Douarre, C.; O'Donohue, M.-F.; Khoury, V. E.; Shin-ya, K.; Morjani, H.; Trentesaux, C.; Riou, J.-F. *J. Biol. Chem.* **2006**, *281*, 38721. (b) Gomez, D.; O'Donohue, M.-F.; Wenner, T.; Douarre, C.; Macadré, J.; Koebel, P.; Giraud-Panis, M. J.; Kaplan, H.; Kolkes, A.; Shin-ya, K.; Riou, J.-F. *Cancer Res.* **2006**, *66*, 6908.
- (6) (a) Huppert, J. L.; Balasubramanian, S. *Nucleic Acids Res.* **2007**, *35*, 406. (b) Huppert, J. L.; Balasubramanian, S. *Nucleic Acids Res.* **2005**, *33*, 2908. (c) Todd, A. K.; Johnston, M.; Neidle, S. *Nucleic Acids Res.* **2005**, *33*, 2901.
- (7) (a) Siddiqui-Jain, A.; Grand, C. L.; Bearss, D.; Hurley, L. H. *Proc. Natl. Acad. Sci. U.S.A.* **2002**, *99*, 11593. (b) Cogoi, S.; Xodo, L. E. *Nucleic Acids Res.* **2006**, *34*, 2536.

- (8) (a) Rankin, S.; Reszka, A. P.; Huppert, J.; Zloh, M.; Parkinson, G. N.; Todd, A. K.; Ladame, S.; Balasubramanian, S.; Neidle, S. *J. Am. Chem. Soc.* **2005**, *127*, 10584. (b) Fernando, H.; Reszka, A. P.; Huppert, J.; Ladame, S.; Rankin, S.; Venkitaraman, A. R.; Neidle, S.; Balasubramanian, S. *Biochemistry* **2006**, *45*, 7854.
- (9) (a) Ou, T. M.; Lu, Y. J.; Huang, Z. S.; Wang, X. D.; Tan, J. H.; Chen, Y.; Ma, D. L.; Wong, K. Y.; Tang, J. C.; Chan, A. S.; Gu, L. Q. *J. Med. Chem.* **2007**, *50*, 1465. (b) Qin, Y.; Rezler, E. M.; Gokhale, V.; Sun, D.; Hurley, L. H. *Nucleic Acids Res.* **2007**, *35*, 1. (c) Bejugam, M.; Sewitz, S.; Shirude, P. S.; Rodriguez, R.; Shahid, R.; Balasubramanian, S. *J. Am. Chem. Soc.* **2007**, *129*, 12926. (d) Sun, D.; Liu, W.-J.; Guo, K.; Rusche, J. J.; Ebbinghaus, S.; Gokhale, V.; Hurley, L. H. *Mol. Cancer Ther.* **2008**, *7*, 880.
- (10) (a) Alberti, P.; Bourdoncle, A.; Saccà, B.; Lacroix, L.; Mergny, J.-L. *Org. Biomol. Chem.* **2006**, *4*, 3383. (b) Xu, Y.; Hirao, Y.; Nishimura, Y.; Sugiyama, H. *Bioorg. Med. Chem.* **2007**, 1275.
- (11) Tang, Z.; Gonçalves, D. P. N.; Wieland, M.; Marx, A.; Hartig, J. S. *ChemBioChem* **2008**, *9*, 1061.
- (12) For a recent review, see: (a) Monchaud, D.; Teulade-Fichou, M.-P. *Org. Biomol. Chem.* **2008**, *6*, 627. For few specific examples, see: (b) Dash, J.; Shirude, P. S.; Balasubramanian, S. *Chem. Commun.* **2008**, 3055. (c) Shirude, P. S.; Gilles, E. R.; Ladame, S.; Godde, F.; Shin-ya, K.; Huc, I.; Balasubramanian, S. *J. Am. Chem. Soc.* **2007**, *129*, 11890. (d) Cian, A. D.; DeLemos, E.; Mergny, J.-L.; Teulade-Fichou, M.-P.; Monchaud, D. *J. Am. Chem. Soc.* **2007**, *129*, 1856. (e) Dixon, I. M.; Lopez, F.; Tejera, A. M.; Estève, J.-P.; Blasco, M. A.; Pratviel, G.; Meunier, B. *J. Am. Chem. Soc.* **2007**, *129*, 1502. (f) Reed, J. E.; Arnal, A. A.; Neidle, S.; Vilar, R. *J. Am. Chem. Soc.* **2006**, *128*, 5992.

Scheme 1. Synthesis of Water Soluble Bis-phenylethynyl Derivatives



G-quadruplex sequences may exist within a genome,⁶ it is now a necessary challenge for chemists to engineer discrimination between G-quadruplexes by small molecules. In principle, there are opportunities to design small molecules that bind through distinct sites, other than the G-tetrad, involving the G-quadruplex loops and grooves, but this has been largely unexplored.¹³

Here we present bis(phenylethynyl) amides meta linked to benzene **9** and 2,6-pyridine **10** that recognize G-quadruplex DNA. Such compounds are neither polycyclic, nor macrocyclic and have free rotation around the triple bond enabling the adoption of all possible twisted and planar conformations of the aryl groups. Owing to their conformational flexibility, we perceived ligands **9** and **10** would offer the potential for modes of G-quadruplex recognition other than the more typical G-tetrad binding site. The lone pair of the pyridine nitrogen atom of **10** and the free amino and amide groups of **9** and **10** have potential to participate in H-bonding interactions with the grooves and loops of the G-quadruplex DNA. In addition, there is potential for electrostatic interactions of the amine side chains with the negatively charged sugar phosphate backbone.

Results and Discussion

Synthesis of Ligands. The water soluble bis-phenylethynyl amides **9** and **10** were efficiently prepared in 64–68% overall yields over 3 steps (Scheme 1). The synthesis involves Pd-mediated Sonogashira coupling¹⁴ of iodoaniline derivative **1** with 1,3-diethynylbenzene (**2**) and 2,6-diethynylpyridine (**3**) in the presence of CuI, Et₃N, and a catalytic amount of PdCl₂(PPh₃)₂ in DMF. The corresponding diester derivatives **4** and **5** were obtained in 78–83% yield.^{12b} Basic hydrolysis of the diester derivatives **4** and **5** afforded the diacids **6** and **7** respectively in excellent yield. The amides **9** and **10** were acquired in 87–90% yield by using chemoselective amide coupling of diacids **6** and

7 with amine **8**. The amide coupling reactions were carried out using EDC, HOBT and *N*-methylmorpholine (NMM) in DMF.

Ligand-Quadruplex Recognition. Ligand-quadruplex recognition was evaluated using a fluorescence resonance energy transfer (FRET) melting assay,¹⁵ surface plasmon resonance (SPR),¹⁶ circular dichroism (CD)^{13,17} and ¹H nuclear magnetic resonance (NMR) spectroscopy.^{18,19} In order to elucidate differential recognition by the small molecule ligands **9** and **10**, we employed the three distinct biologically relevant promoter G-quadruplex DNA targets *c-myc*,^{7a} *c-kit1*,^{8a} *c-kit2*,^{8b} and a duplex DNA (dup) as a control.

Fluorescence Resonance Energy Transfer (FRET) Melting Assay. FRET melting analysis determines the ligand-induced stabilization of a folded quadruplex by measurement of the ligand induced shift in the melting temperature (ΔT_m).¹⁵ The FRET melting data, obtained using dual-labeled sequences, is

- (13) White, E. W.; Taniou, F.; Ismail, M. A.; Reszka, A. P.; Neidle, S.; Boykin, D. W.; Wilson, W. D. *Biophysical Chemistry* **2007**, *126*, 140.
 (14) For reviews, see: (a) Sonogashira, K. In *Metal-Catalyzed Cross-coupling Reactions*; Diederich, F., Stang, P. J., Eds.; Wiley-VCH: Weinheim, Germany, 1998; pp 203–229. (b) Negishi, E.-I.; Anastasia, L. *Chem. Rev.* **2003**, *103*, 1979.

- (15) (a) Darby, R. A. J.; Sollogoub, M.; McKeen, C.; Brown, L.; Risitano, A.; Brown, N.; Barton, C.; Brown, T.; Fox, K. R. *Nucleic Acids Res.* **2002**, *30*, e39. (b) Cian, A. De.; Guittat, L.; Kaiser, M.; Sacca, B.; Amrane, S.; Bourdoncle, A.; Alberti, P.; Teulade-Fichou, M.-P.; Lacroix, L.; Mergny, J.-L. *Methods* **2007**, *42*, 183.
 (16) (a) Teulade-Fichou, M.-P.; Carrasco, C.; Guittat, L.; Bailly, C.; Alberti, P.; Mergny, J.-L.; David, A.; Lehn, J.-M.; Wilson, W. D. *J. Am. Chem. Soc.* **2003**, *125*, 4732. (b) Schouten, J. A.; Ladame, S.; Mason, S. J.; Cooper, M. A.; Balasubramanian, S. *J. Am. Chem. Soc.* **2003**, *125*, 5594.
 (17) (a) Paramasivan, S.; Rujan, I.; Bolton, P. H. *Methods* **2007**, *43*, 324. (b) Balagurumorthy, P.; Brahmachari, S. K. *J. Biol. Chem.* **1994**, *269*, 21858. (c) Jin, B.; Gaffney, L.; Wang, C.; Jones, R. A.; Breslauer, K. J. *Proc. Natl. Acad. Sci. U.S.A.* **1992**, *89*, 8832.
 (18) (a) Patel, D. J.; Phan, A. T.; Kuryavyi, V. *Nucleic Acids Res.* **2007**, *35*, 7429. (b) Silva, M. *Webba da Methods* **2007**, *43*, 264. (c) Phan, A. T.; Kuryavyi, V.; Gaw, H. Y.; Patel, D. J. *Nat. Chem. Biol.* **2005**, *1*, 167. (d) Patel, D. J.; Phan, A. T. *J. Am. Chem. Soc.* **2003**, *125*, 15021. (e) Read, M. A.; Neidle, S. *Biochemistry* **2000**, *39*, 13422. (f) Gavathiotis, E.; Heald, R. A.; Stevens, M. F. G.; Searle, M. S. *Angew. Chem., Int. Ed.* **2001**, *40*, 4749. (g) Fedoroff, O. Y.; Salazar, M.; Han, H.; Chemeris, V. V.; Kerwin, S. M.; Hurley, L. H. *Biochemistry* **1998**, *37*, 12367.
 (19) (a) Martino, L.; Virno, A.; Pagano, B.; Virgilio, A.; Di Micco, S.; Galeone, A.; Giancola, C.; Bifulco, G.; Mayol, L.; Randazzo, A. *J. Am. Chem. Soc.* **2007**, *129*, 16048. (b) Cocco, M. J.; Hanakahi, L. A.; Huber, M. D.; Maizels, N. *Nucleic Acids Res.* **2003**, *31*, 2944. (c) Randazzo, A.; Galeone, A.; Mayol, L. *Chem. Commun.* **2001**, 1030.

Table 1. G-Quadruplex Stabilization (ΔT_m) Potential by FRET-Melting and Dissociation Constants (K_d) Measured by SPR

Ligand	c-myc (77 ± 1) ^a	c-kit2 (71 ± 1) ^a	c-kit1 (57 ± 1) ^a	dup (58 ± 1) ^a
ΔT_m at 1 μ M conc. (°C)				
9	2.9	6.0	8.9	0.2
10	7.3	9.2	13.5	0.2
K_d [μ M] and stoichiometry (<i>n</i>)				
9	2.68 ± 0.06 (2:1)	4.44 ± 0.55 (2:1)	9.65 ± 0.41 (2:1)	nd ^b
10	0.57 ± 0.02 (2:1)	0.69 ± 0.03 (1:1)	3.04 ± 0.08 (2:1)	nd ^b

^a T_m in 60 mM potassium cacodylate buffer, pH 7.4 without ligand.

^b No significant binding up to 25 μ M.

summarized in Table 1 (Figure 1). Both ligands showed moderate stabilization for G-quadruplexes (ΔT_m ranging from 3–13 °C) with no detectable stabilization of duplex DNA. Ligand **10** exhibits good stabilization potential ($\Delta T_m = 7.3$ °C, i.e. a T_m of 84 °C) for the c-myc quadruplex at 1 μ M ligand concentration (Figure 1B). The stabilization potential for c-kit2 by ligand **10** was found out to be 9.2 °C at 1 μ M (i.e., $T_m = 80$ °C). The observed ΔT_m of ligand **10** for c-kit1 was 13.5 °C (i.e., $T_m = 71$ °C) at 1 μ M concentration. Ligand **9** exhibits a stabilization potential of 2.9 °C for c-myc, 6.0 °C for c-kit2 and 8.9 °C for c-kit1 quadruplex at 1 μ M concentration (Figure 1A, Table 1). It is interesting to note that ligands, **9** and **10** both show very high preference for stabilizing G-quadruplex DNA over duplex DNA.

Surface Plasmon Resonance (SPR). While FRET melting analysis provides a measure of the ligand-induced stabilization of a folded quadruplex, SPR measures equilibrium binding. It is noteworthy in SPR analysis that ligands show high affinity for G-quadruplex motifs (Table 1, Figure 2). The dissociation constant of ligand **10** for c-myc quadruplex DNA ($K_d = 570$ nM) is comparable with the data obtained for one of the best reported quadruplex ligands Se2SAP ($K_d = 620$ nM for one of the c-myc sequence).²⁰ Similarly the K_d of ligand **10** for the c-kit1 quadruplex (3.04 μ M) compared favorably with the best ligands (4.90 μ M) from our recently reported isoalloxazine series.^{9c} Ligand **10** also binds to c-kit2 quadruplex with 1:1 stoichiometry and a submicromolar equilibrium dissociation constant ($K_d = 690$ nM). A 2:1 stoichiometry was found for ligand **10** with c-myc and c-kit1 quadruplex targets, suggestive of more than one mode of binding (Table 1, Figure 2B). Ligand **9** was found to bind c-myc, c-kit2 and c-kit1 with dissociation constants (K_d) of 2.68, 4.44 and 9.65 μ M, respectively (Table 1, Figure 2A). Ligands **9** and **10** show 1–2 fold selectivity for c-myc over c-kit2, and 4–6 fold for c-myc over the c-kit1 quadruplex (Table 1).

The correlation between stabilization (ΔT_m) and equilibrium binding (K_d) is not straightforward and thus there is no simple relationship between ΔT_m and K_d . However, for ligands **9** and **10** the trend for the K_d values obtained by SPR and G-quadruplex stabilization effects as determined by FRET (Table 1), for a given quadruplex target were consistent with the tightest binder (i.e., lower K_d) also inducing better thermal stabilization (i.e., larger ΔT_m). For ligands **9** and **10** no detectable binding to duplex DNA was observed by SPR, which was consistent with very low ΔT_m values by FRET melting, and confirms the high selectivity for G-quadruplex DNA (Table 1). Ligand **10** binds c-kit2 with an apparent stoichiometry of 1:1

as compared to 2:1 for c-myc and c-kit1. This distinction may reflect the differences in binding sites between the three quadruplexes, each of which has a unique configuration of loop sequences. A clear outcome is that ligand **10** with a central pyridine ring shows higher stabilization temperatures and binding affinities compared to the benzene analogue **9** (Table 1, Figures 1 and 2).

CD and NMR Spectroscopic Study of c-kit2 DNA G-quadruplex. CD spectroscopy^{13,17} and ¹H NMR^{18,19} spectroscopy can reveal the preference of ligands to induce or recognize a particular quadruplex structure and can provide some insights into the binding mode of ligands. To examine the fundamental properties of G-quadruplex recognition we carried out ligand binding studies with and without stabilizing salt. The CD spectrum of c-kit2 suggests that, in the absence of any added salt, it exists as a mixture of a parallel structure,^{8b} with a major positive peak at 263 nm, and a small proportion of an antiparallel conformation as indicated by a minor peak at 295 nm (Figure 3A). Similarly the ¹H NMR spectrum of c-kit2 reveals two sets of imino proton resonances in the region of the spectrum characteristic of G-tetrad formation; one cluster at δ 10.8–12 ppm^{18a} and the other more dispersed at δ 9.6 and 12.3–13.8 ppm (Figure 4A). Based on the corresponding CD spectral data for c-kit2 under similar salt and pH conditions, we attribute that these imino proton resonances of c-kit2 corresponds to parallel and antiparallel conformations. We performed a real time titration of ligand **10** with c-kit2 quadruplex forming sequences, in the absence of added salt, monitored by CD and NMR spectroscopy (Figures 3 and 4). Upon each addition of ligand **10** to c-kit2 quadruplex there are noteworthy changes in the CD spectrum that involve an increase in ellipticity at 263 nm, with the disappearance of signal at 295 nm. This is consistent with the induction of a predominantly parallel conformation of the c-kit2 quadruplex by ligand **10** (Figure 3A).²¹ In the corresponding NMR experiment addition of ligand **10** to c-kit2 results in a concomitant decrease in intensity of the dispersed set of signals at δ 9.6 and 12.3–13.8 ppm, and an increase in intensity of the clustered set of signals at δ 10.8–12 ppm. The imino proton resonances of c-kit2, in the presence of K⁺, are only observed in the region of δ 10.8–12 ppm (bottom spectra in red, Figure 4A), supporting our assertion that ligand **10** favors the parallel conformation. We have recently determined the dominant topology of c-kit2, in the presence of K⁺, as a parallel conformation by multidimensional ¹H NMR spectroscopy.²² In line with the structural information, the CD spectra of c-kit2 shows existence of a predominantly parallel conformation^{8b} in the presence of K⁺ and ligand induced CD spectral changes were less prominent (Figure 3B). Upon addition of excess ligand (up to 10 mol equiv) to c-kit2, a slight increase in ellipticity at 263 nm was observed.

Mode of Binding. When an achiral ligand binds to DNA, a positive ICD signal has been taken as an indicator of groove binding to duplex^{23,24} and to quadruplex^{13,25} structures. In the CD spectroscopic analysis with c-kit2 (Figure 3), besides the

(21) Since the absorbance of achiral **10** (263, 351 nm) also overlaps at 263 nm, we can not rule out the contribution of ICD signal (at 263 nm) due to the chirality transfer of DNA to the ligand.

(22) Hsu, S.-T. D.; et al. Unpublished results.

(23) Eriksson, M.; Nordén, B. *Methods Enzymol.* **2001**, *340*, 68.

(24) (a) Hranjec, M.; Piantanida, I.; Kralj, M.; Šuman, L.; Pavelić, K.; Karminski-Zamola, G. *J. Med. Chem.* **2008**, *51*, 4899. (b) Catoen-Chackal, S.; Facompré, M.; Houssin, R.; Pommery, N.; Goossens, J.-F.; Colson, P.; Bailly, C.; Hélichart, J.-P. *J. Med. Chem.* **2004**, *47*, 3665.

(20) Seenisamy, J.; Bashyam, S.; Gokhale, V.; Vankayalapati, H.; Sun, D.; Siddiqui-Jain, A.; Streiner, N.; Shin-ya, K.; White, E.; Wilson, W. D.; Hurlay, L. H. *J. Am. Chem. Soc.* **2005**, *127*, 2944.

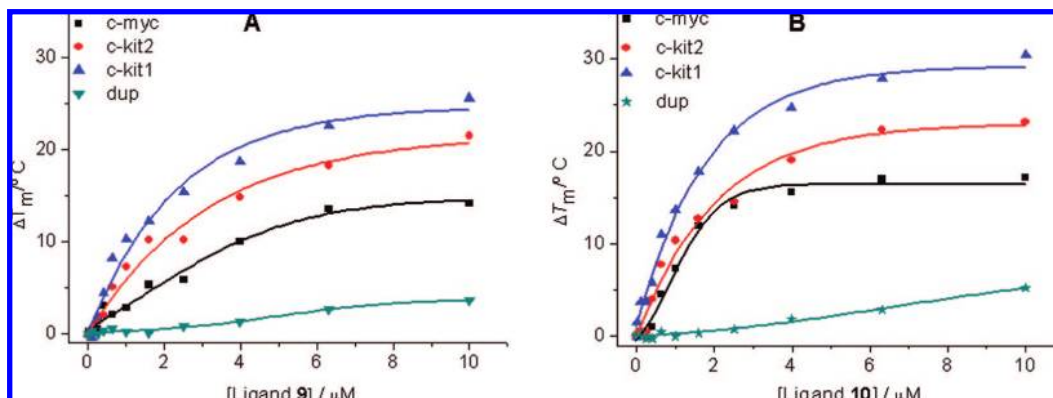


Figure 1. FRET stabilization curves for ligand **9** (A) and ligand **10** (B) upon binding to c-myc, c-kit2, c-kit1, and dup DNA (buffer: 60 mM potassium cacodylate pH 7.4).

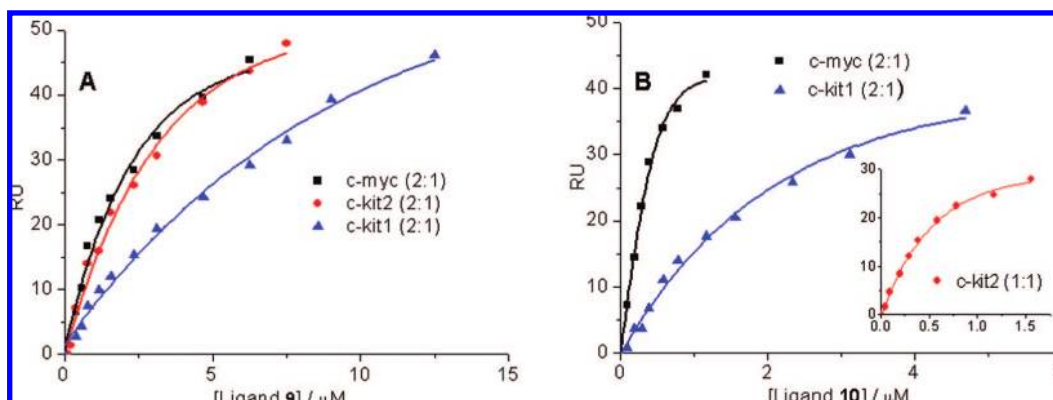


Figure 2. SPR binding curves for ligand **9** (A) and ligand **10** (B) binding to c-myc, c-kit2, and c-kit1 (running buffer: 50 mM Tris-HCl pH 7.4, 100 mM KCl).

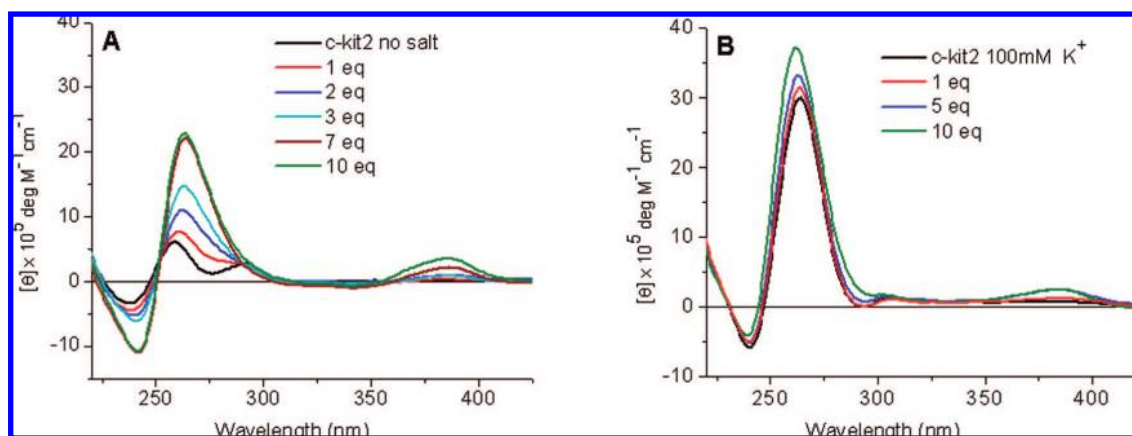


Figure 3. CD spectra of a solution of 12.5 μM c-kit2 in Tris buffer (pH 7.4), in the absence (A) and presence (B) of added salt, 0–10 equiv of ligand **10**.

ligand dependent increase in ellipticity at 263 nm²¹ we also observed the appearance of a red-shifted induced signal (ICD) at 380 nm. A bathochromic shift of 30 nm was also observed in the UV/vis titration of ligand **10** with the c-kit2 G-quadruplex forming sequence (see Supporting Information, S.I.). A similar CD titration of **10** with c-myc quadruplex also revealed induction of a parallel quadruplex structure and an ICD band at 380 nm (S.I.). An ICD band at 380 nm was also observed

upon titration of **10** with the c-kit1 quadruplex, but with no significant increase in ellipticity at 263 nm²¹ (parallel structure, S.I.).²⁶ The positive ICD signal shown by binding of **10** to c-kit2 (Figure 3), c-myc (S.I.) and c-kit1 (S.I.) is suggestive of a groove binding mode in the quadruplex, and is consistent with our design hypothesis which did not necessarily target G-tetrad recognition.

(25) (a) Yamashita, T.; Uno, T.; Ishikawa, Y. *Bioorg. Med. Chem.* **2005**, *13*, 2423. (b) Sun, H.; Tang, Y.; Xiang, J.; Xu, G.; Zhang, Y.; Zhang, H.; Xu, L. *Bioorg. Med. Chem. Lett.* **2006**, *16*, 3586.

(26) An apparent quadruplex unfolding was observed for c-kit1 quadruplex upon addition of ligand **10** (at higher concentration than the K_d) in the presence of K^+ (see S.I.).

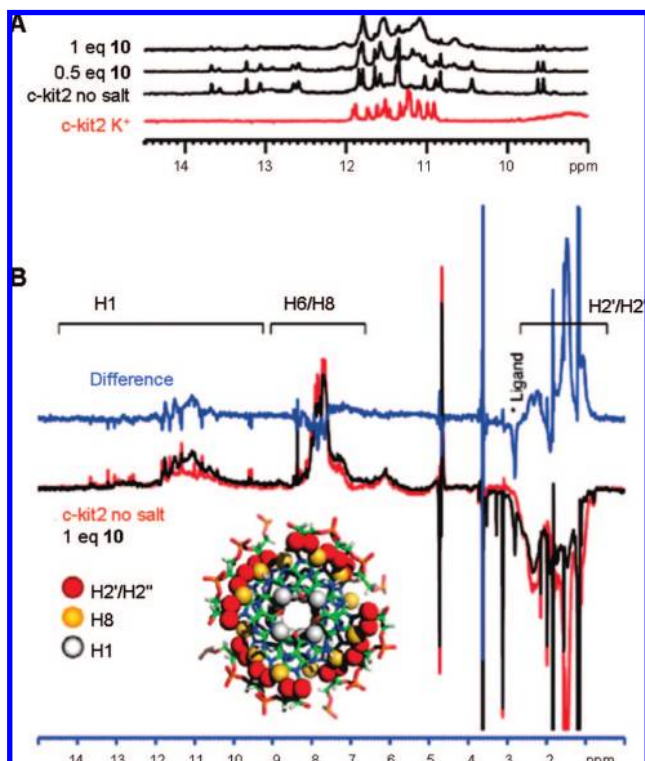


Figure 4. NMR titration study of a solution of 260 μM c-kit2 complexed with ligand **10**; (A) the imino proton spectra of c-kit2 with 0, 0.5, 1 equiv of ligand **10** in the absence of added salt; bottom spectra (red) shows the imino proton spectrum of c-kit2 in presence K^+ . (B) 1D jump-and-return ^1H NMR spectra of c-kit2 in the absence (red) and in the presence (black) of 1 equiv of ligand **10** without added salt; the difference spectrum of the two is shown in blue with regions of different proton types indicated above; inset: a top view of a molecular model of three-layer G-tetrad in a parallel conformation²² with $\text{H}2'/\text{H}2''$, H8 and H1 protons shown in red, gold and gray spheres.

To gain further insights into the structural basis of the c-kit2 recognition by ligand **10**, we carried out NMR titration experiments by adding ligand **10** into a solution containing 260 μM of c-kit2 in H_2O to monitor structural changes upon ligand binding. Due to ring current shielding, the imino proton resonances of G-quadruplexes have been reported to undergo significant upfield chemical shift changes upon small molecules binding by end stacking onto the G-tetrad.^{18b-d,f} However, in our case, upon titration of ligand **10**, the imino resonances at δ 10.8–12 ppm in the ^1H NMR spectra, which correspond to a parallel conformation, exhibit significant line-broadening without marked upfield shifts, while concomitant disappearance of another set of the more dispersed imino proton resonances at δ 12.5–14 ppm are observed (Figure 4A, B and S.I.). The absence of upfield-shifted chemical shift changes is consistent with a mode of binding by ligand **10** that is *not* via G-tetrad stacking. By comparing the full ^1H NMR spectra of free and liganded c-kit2 in the absence of added salt, we found similar line broadening in other regions of the liganded spectrum of c-kit2 but with negligible chemical shift changes. Note that the line broadening, indicative of restricted motions upon ligand binding, is most pronounced for the ribose protons $\text{H}2'/\text{H}2''$, which are located in the proximity of the grooves of G-tetrads (Figure 4B). Such differential line-broadening has also been reported for distamycin A, a common DNA groove-binder, binding to the grooves of a parallel G-quadruplex^{19a} and such groove binding also induces negligible chemical shift changes of the

H8 protons in the G-tetrad, which argues against end-stacking to a G-tetrad.^{19b} In addition, we also observe some degrees of protection for the amino protons of c-kit2, which also reside in the groove region and may be sequestered from solvent exchange in the presence of ligand **10**, as evidenced by the presence of some very broad amino proton (NH_2) correlations in the 2D NOESY spectrum; such correlations are completely absent in the spectrum of free c-kit2 (S.I.). Together, these NMR spectroscopic data strongly support groove binding mode for ligand **10**.

Experimental Section

Chemistry. All experiments were carried out under inert atmosphere unless otherwise stated. ^1H NMR spectra were recorded at 500 MHz using Bruker DRX 500 instrument. ^1H spectra were recorded in deuterated solvents as detailed. Chemical shifts are reported in parts per million (ppm) and are referenced to the residual solvent peak. The following abbreviations are used: s, singlet; d, doublet; t, triplet; q, quartet; m, multiplet; br, broad. Data are reported in the following manner: chemical shift (multiplicity, coupling constant if appropriate, integration). Coupling constants (J) are reported in Hertz to the nearest 0.5 Hz. ^{13}C NMR spectra were recorded at 125 MHz using Bruker DRX 500 instrument. Flash column chromatography (FC) was performed using Merck Kieselgel 60 (40–63 mm, 230–40 mesh) silica gel. Thin layer chromatography were carried out on glass plates precoated with Merck silica gel 60 F254 which were visualized either by quenching of UV fluorescence or by dipping in a $\text{KMnO}_4/\text{H}_2\text{O}$ solution followed by heat, as appropriate. Melting points were recorded using a Griffin melting point apparatus and are uncorrected. Mass spectra were recorded on Micromass Q-ToF (ESI) or Kratos Concept (EI) spectrometers. HPLC was performed using a varian pursuit C18 5 μ column (250 \times 10 mm) and a gradient elution with 0.1% TFA/MeCN and 0.1% TFA/ H_2O at a flow rate of 12 mL/min. Unless otherwise noted, all materials were obtained from commercial suppliers and used without further purification.

Synthesis, General Procedures: Sonogashira Coupling. A reaction flask containing iodoaniline derivative **1** (2 equiv), diethynyl compounds **2** or **3** (1 equiv), $\text{PdCl}_2(\text{PPh}_3)_2$ (10 mol%), and CuI (20 mol%) was evacuated and filled with argon. To the mixture DMF (5 mL/1 mmol) and triethylamine (10 equiv) were added. After stirring at rt under an argon atmosphere for 9 h, the mixture was quenched with water and extracted with 3 \times ethylacetate. The combined organic solution was washed with 1 \times brine, dried with Na_2SO_4 and removed *in vacuo*. The residue was purified by chromatography on silica gel to afford the corresponding cross coupled product **4** or **5**.

Hydrolysis of Esters. NaOH (10 equiv, 2N solution in water) was added to a solution of the methyl ester **4** or **5** (1 equiv) in methanol and THF (1:1) at 0 $^\circ\text{C}$. After stirring for 12 h at rt, the reaction mixture was removed *in vacuo* and the residue was dissolved in water. After washing with EtOAc, the aqueous phase was acidified with formic acid and subsequently extracted with 3 \times EtOAc. The combined organic layers were dried with Na_2SO_4 . Removal of the solvent provided the crude product **6** or **7**, which was used without further purification.

Amide Coupling. A mixture of dicarboxylic acid **6** or **7** (0.25 mmol), EDC (1.06 mmol, 4.24 equiv), HOBt (1.06 mmol, 4.24 equiv), NMM (2.10 mmol, 8.40 equiv), amine **8** (0.78 mmol, 3.12 equiv) in DMF (5 mL) was stirred at rt for 10 h. The solvent was removed *in vacuo* and purified by HPLC (gradient: starting from $\text{H}_2\text{O}:\text{MeCN}$ (1% TFA) 20:80 to pure MeCN (1% TFA) over 35 min, 12 mL/min, provided the desired compounds **9** or **10**.

Diester Derivative 4. Yield (78%); colorless solid; 152–153 $^\circ\text{C}$; ^1H NMR (CDCl_3): δ = 8.07 (d, J = 1.7 Hz, 2H), 7.81 (dd, J = 8.56, 1.0 Hz, 2H), 7.66 (s, 1H), 7.47–7.45 (m, 2H), 7.35–7.30 (m, 1H), 6.69 (d, J = 8.6 Hz, 2H), 4.72 (s, 4H), 3.85 (s, 6H); ^1H NMR (d_6 -DMSO): δ = 8.00 (m, 1H), 7.83 (d, J = 2.0 Hz, 2H),

7.66–7.64 (m, 4H), 7.44 (t, $J = 7.5$ Hz, 1H), 6.76 (d, $J = 8.7$ Hz, 2H), 6.45 (s, 4H), 3.76 (s, 6H); ^{13}C NMR (d_6 -DMSO): $\delta = 165.7$, 153.8, 134.2, 134.1, 131.3, 131.2, 128.9, 123.2, 116.3, 113.4, 104.5, 93.4, 86.3, 51.6; HRMS (ESI): calcd for $\text{C}_{26}\text{H}_{20}\text{N}_2\text{O}_4$ [$\text{M} + \text{H}$] $^+$ 424.1422, found 424.1418.

Diester Derivative 5. Yield (83%); colorless solid; 136–138 °C; ^1H NMR (CDCl_3): $\delta = 7.92$ (t, $J = 7.6$ Hz, 1H), 7.89 (d, $J = 2.0$ Hz, 2H), 7.81 (d, $J = 7.9$ Hz, 2H), 7.70 (d, $J = 8.6$, 2.0 Hz, 2H), 6.80 (d, $J = 8.8$ Hz, 2H), 6.47 (br, 4H), 3.77 (s, 6H); ^{13}C NMR (d_6 -DMSO): $\delta = 165.6$, 154.1, 142.9, 137.4, 134.6, 131.9, 126.8, 116.5, 113.7, 103.5, 93.3, 85.8, 51.6; HRMS (ESI): calcd for $\text{C}_{25}\text{H}_{19}\text{N}_3\text{O}_4$ [$\text{M} + \text{H}$] $^+$ 426.1459, found 426.1442; [$\text{M} + \text{Na}$] $^+$ 448.1278, found 448.1264.

Dicarboxylic Acid Derivative 6. Yield (94%); light brown solid; 271–271 °C (decomp); yield ^1H NMR (d_6 -DMSO): $\delta = 8.07$ (d, $J = 1.7$ Hz, 1H), 7.84 (d, $J = 1.9$ Hz, 2H), 7.67–7.64 (m, 4H), 7.5 (d, $J = 8.7$ Hz, 1H), 6.76 (d, $J = 8.0$ Hz, 2H), 6.33 (s, 4H); OH could not be detected; ^{13}C NMR (d_6 -DMSO): $\delta = 167.2$, 153.8, 134.6, 134.5, 131.9, 131.5, 129.3, 123.6, 118.0, 113.6, 104.8, 93.6, 86.9; HRMS (ESI): calcd for $\text{C}_{24}\text{H}_{16}\text{N}_2\text{O}_4$ [$\text{M} + \text{Na}$] $^+$ 419.1002, found 419.1021.

Dicarboxylic Acid Derivative 7. Yield (91%); orange solid; mp 272–274 °C (decomp); ^1H NMR (d_6 -DMSO): $\delta = 7.89$ (dd, $J_1 = 7.1$ Hz, 1H), 7.87 (d, $J = 2.0$ Hz), 7.78 (d, $J = 7.9$ Hz, 2H), 7.68 (dd, $J = 8.7$, 2.1 Hz, 2H), 6.78 (d, $J = 8.7$ Hz, 2H), 6.39 (s, 4H), OH could not be determined; ^{13}C NMR (d_6 -DMSO): $\delta = 166.8$ (s), 153.9, 143.1, 137.2, 134.6, 132.1, 126.7, 117.8, 113.5, 103.4, 93.3, 85.8; HRMS (ESI): calcd for $\text{C}_{23}\text{H}_{15}\text{N}_3\text{O}_4$ [$\text{M} + \text{H}$] $^+$ 398.1146, found 398.1131.

Bis-phenylethynyl Amide Derivative 9. Yield (87%); light yellow oil; ^1H NMR (CD_3CN): $\delta = 9.26$ (s, 2H), 7.85 (d, $J = 2.1$ Hz, 1H), 7.81–7.80 (m, 1H), 7.62 (dd, $J = 8.7$, 2.2 Hz, 2H), 7.58 (dd, $J = 7.7$, 1.6 Hz, 2H), 7.44 (td, $J = 8.0$, 0.4 Hz, 1H), 3.43 (q, $J = 6.1$ Hz, 4H), 3.06 (q, $J = 6.1$ Hz, 4H), 3.08 (q, $J = 5.9$ Hz, 2H), 2.82 (s, 6H), 2.81 (s, 6H), 1.98–1.95 (m, 4H); ^{13}C NMR (CD_3CN): $\delta = 169.6$, 153.2, 134.9, 133.0, 132.2, 130.4, 130.0, 124.4, 122.1, 114.3, 106.6, 94.5, 86.7, 55.6, 43.5, 36.3, 25.8; HRMS (ESI): calcd for $\text{C}_{34}\text{H}_{41}\text{N}_6\text{O}_2$ [$\text{M} + \text{H}$] $^+$ 565.3286, found 565.3306.

Bis-phenylethynyl Amide Derivative 10. Yield (90%); yellow solid, mp 92–93 °C; ^1H NMR (CD_3CN): $\delta = 9.30$ (s, 2H), 7.96 (t, $J = 7.7$ Hz, 1H), 7.95 (d, $J = 2.1$ Hz, 2H), 7.71–7.69 (m, 4H), 6.87 (d, $J = 7.5$ Hz, 2H), 3.49 (sex, $J = 5.2$ Hz, 4H), 3.46 (dt, $J = 6.2$, 5.9 Hz, 4H), 3.08 (q, $J = 5.9$ Hz, 4H), 2.87 (s, 6H), 2.86 (s, 6H), 2.09–1.94 (m, 4H); ^{13}C NMR (CD_3CN): $\delta = 169.5$, 153.9, 143.0, 139.5, 133.5, 131.4, 127.8, 122.1, 114.6, 104.9, 93.2, 88.2, 55.5, 43.5, 36.1, 25.9; HRMS (ESI): calcd for $\text{C}_{34}\text{H}_{40}\text{N}_6\text{O}_2$ [$\text{M} + \text{H}$] $^+$ 566.3238, found 566.3223.

Fluorescence Resonance Energy Transfer (FRET) Assay. All the oligonucleotides and their fluorescent conjugates (Eurogentec, Southampton, UK) were initially dissolved as a 100 μM stock solution in purified water; further dilutions were carried out in the relevant buffer. The ability of the compounds to stabilize G-quadruplex DNA was investigated using a fluorescence resonance energy transfer (FRET) assay modified to be used as a high-throughput screen in a 96-well format. We have used four different labeled oligonucleotides comprised of c-kit1: *FAM*-d(GGGA-GGGCGCTGGGAGGAGGG)-*TAMRA*, c-kit2: *FAM*-d(GGGC-GGGCGAGGGAGGGG)-*TAMRA*, c-myc: *FAM*-d(TGAGGGT-GGGTAGGGTGGGTAA)-*TAMRA* and a duplex DNA *FAM*-d(TATAGCTATA-HEG-TATAGCTATA)-*TAMRA*; donor fluorophore *FAM* is 6-carboxyfluorescein; acceptor fluorophore *TAMRA* is 6-carboxytetramethyl-rhodamine. As a typical experiment, the oligonucleotides were prepared as a 400 nM solution in a 60 mM potassium cacodylate buffer (pH 7.4) and then annealed by heating to 90 °C for 2 min, followed by cooling to room temperature. Compounds were stored at –80 °C and dilutions were done with 60 mM potassium cacodylate buffer (pH 7.4). One mM stock solution of ligands **9** and **10** were made up in MQ water. The 96-well plates (MJ Research, Waltham, MA) were prepared by

aliquoting 50 μL of the annealed DNA into each well, followed by 50 μL of the compound solutions using Beckman Coulter liquid-handling robot. For each compound, a minimum of 10 different concentrations were tested. Fluorescence melting curves were determined in a Roche light cycler 480, using a total reaction volume of 100 μL . Measurements were made in duplicate with excitation at 483 nm and detection at 533 nm. Final analysis of the data was carried out using Origin 7.5 (OriginLab Corp., Northampton, MA) and shown in Figure 1.

Surface Plasmon Resonance. Surface plasmon resonance measurements were performed on a four-channel Biacore 3000 optical biosensor system (Biacore Inc.) using a streptavidin-coated sensor chip (Biacore SA-chip). We have used four biotinylated G-quadruplex forming sequences comprised of c-myc promoter G-quadruplex DNA, c-myc d(*biotin*-[TGAGGGTGGGTAGGGT-GGGTAA]) and the two c-kit promoter G-quadruplex DNA, c-kit1 d(*biotin*-[AGGGAGGGCGCTGGGAGGAGGG]) and c-kit2 d(*biotin*-[CCCGGGCGGGCGCGAGGGAGGGGAGGG]). We have also used a duplex DNA d(*biotin*-[GGGCATAGTGCCTGGCGGTT-TAGC]) hybridized with its complementary sequence as a non-quadruplex control. The DNA oligonucleotides were folded in filtered and degassed running buffer (Tris-HCl 50 mM pH 7.4, 100 mM KCl; 95 °C for 5 min then cooled to room temperature overnight) and immobilized (500 RU) in flow cells 2, 3 and 4, leaving the first flow cell empty as a blank. DNA binding experiments were carried out with running buffer at a flow rate of 20 $\mu\text{L min}^{-1}$. Ligand solutions **9** and **10** were freshly prepared with running buffer by serial dilutions from stock solutions. These solutions were injected using the KINJECT command (Biacore 3000 Control Software version 3.0.1) for 2 min followed by a 30 s 1 M KCl injection and a 30 s running buffer injection for chip regeneration. Each sample injection was repeated in duplicate. The response at equilibrium (R_{eq}) was plotted against concentration of analyte to generate a hyperbolic binding curve. The final graphs were obtained by subtracting blank sensorgrams from the duplex or quadruplex sensorgrams. For ligands **9** and **10** dissociation constants were determined by fitting the binding curve using the steady state affinity algorithm (Biaevaluation 3.0.2).

Circular Dichroism (CD). Circular dichroism (CD) spectroscopy was used to elucidate ligand effects on the promoter intramolecular G-quadruplex sequences in the presence and absence of added salt (K^+). CD spectra were recorded on a Applied Photophysics Chirascan Circular Dichroism Spectrophotometer (Applied Photophysics Ltd., UK) using a quartz cell of 1-mm optical path length and an instrument scanning speed of 100 nm/min with a response time of 2 s, and over a wavelength range of 200–330 nm and 200–450 nm. We used three different G-quadruplex forming oligonucleotides in the study, the two c-kit promoter G-quadruplex DNA; c-kit1 d(GGGAGGGCGCTGGGAGGGAGGG) and c-kit2 d(GGGCGGGCGCGAGGGAGGGG) and c-myc promoter G-quadruplex DNA; c-myc d(TGAGGGTGGGTAGGGTGGGTAA). All DNA samples were dissolved in Tris buffer (50 mM, pH 7.4). Where appropriate, the samples also contained 100 mM KCl. Ligand **10** (1 mM solution with MQ water) was titrated into the DNA samples at 1 mol equiv up to 10 mol equivs. The DNA strand concentrations used were 12.5 μM , and the CD data are a representation of three averaged scans taken at 23 °C. All CD spectra are zero corrected and baseline-corrected for signal contributions due to the buffer.

NMR Experiments. ^1H NMR spectra of c-kit2 were recorded at 298K (700 MHz Bruker Avance spectrometer equipped with a cryogenic TXI probe) with jump and return water suppression to minimize saturation of labile proton signals.^{18a} The titration experiments started with 500 μL of 260 μM c-kit2 DNA G-quadruplex d[CGGGCGGGCGCGAGGGAGGGG] in 20 mM Tris buffer, pH 7.4 and aliquots of compound **10** (5 mM in the same

buffer) were added in steps to yield 0–2 equiv (S.I.). NMR spectra were recorded immediately after individual titration steps.

Conclusion

In summary we have identified bis-phenylethynyl amide derivatives as a potent G-quadruplex binding small molecule scaffold. These ligands show very good binding affinity, excellent quadruplex:duplex selectivity and also promising discrimination between intramolecular promoter quadruplexes. Our data suggests, such compounds induce parallel G-quadruplex structure and have potential for G-quadruplex groove recognition. We believe that the modes of G-quadruplex recognition other than via the G-tetrad stacking should be seriously considered for second generation ligands. The biological properties of these molecules are currently under investigation.

Acknowledgment. We thank the BBSRC for project grant funding, Cancer Research UK for programme funding and the European Commission (Marie Curie Incoming Postdoctoral Fellowship to J.D. for funding). S.T.D.H. is a recipient of a Netherlands Ramsay Memorial Fellowship and a Human Frontier Science Program Long-term Fellowship (LT00798/2005). We thank Raphaël Rodriguez and Zoë A. E. Waller for useful discussions relating to the SPR experiments.

Supporting Information Available: CD, UV and NMR spectroscopic data. This material is available free of charge via the Internet at <http://pubs.acs.org>.

JA8046552